Two baseflow separation methods based on daily average gage height and discharge

Weifei Yang, Changlai Xiao, Xiujuan Liang and Zhihao Zhang

ABSTRACT

Hydrologists are urgently seeking to find a more universal and inexpensive tracer for baseflow separation, and gage height may form an appropriate choice. This study derives the gage height mass balance (GHMB) and gage height power function (GHPF) methods using a two-component mass balance equation based on the relationship between the gage height and streamflow. The GHMB and GHPF methods are corrected by comparing the results of the conductivity mass balance (CMB), conductivity power function (CMBPF), GHMB, and GHPF methods in 20 basins in the United States. Subsequently, the corrected GHMB and GHPF methods are applied to seven other basins. The results indicate that: (1) the baseflow index (BFI) values calculated from the GHMB and GHPF methods are in good agreement with those of conventional methods; (2) the daily baseflow calculated as per the GHMB and GHPF methods can be suitably fitted with the CMB method; (3) the baseflow is significantly suppressed when the flood peak is larger, and deviations between the GHMB, GHPF, and CMB results are mainly observed for flood events with a large flood peak. As a tracer, the gage height can reasonably separate the baseflow, and the results indicate the efficacy of the methods.

Key words | baseflow separation, gage height, mass balance, power function, tracer

Weifei Yang
Changlai Xiao
Xiujuan Liang (corresponding author)
Zhihao Zhang
Key Laboratory of Groundwater Resources and Environment, Ministry of Education and Key Laboratory of Water Resources and Aquatic Environment, College of New Energy and Environment,
Jilin University,
Changchun 130021,
China
E-mail: *lax64@126.com*

INTRODUCTION

Streamflow refers to the flow of water in streams, rivers, and other channels, and it forms a major element of the water cycle. Streamflow is usually divided into surface runoff and baseflow, where baseflow is the groundwater contribution to streamflow. Water resource management, groundwater resource calculations, and hydrogeological modeling all require reasonable estimations of the baseflow (Zhang *et al.* 2014; Saraiva Okello *et al.* 2018). Saraiva Okello *et al.* (2018) quantified runoff components in a semi-arid mesoscale catchment in South Africa using a tracer-based hydrograph separation method and digital filters. Bastola *et al.* (2018) identified the annual and monthly contributions of baseflow to streamflow in Nepal using three different separation methods. Bahrami *et al.* (2019) studied the effect of different baseflow separation methods on flood hydrograph simulation, etc. Thus, it is important to use a suitable method for baseflow separation.

There are many kinds of baseflow separation methods, which can be divided into three categories according to the different separation mechanisms involved. The first category involves the time-step methods, which usually divide streamflow sequences into several small units according to a certain time-step N, and subsequently, the minimum value in each unit is selected to obtain the baseflow via linear interpolation. Such methods mainly include the BFI method (Wahl & Wahl 1988), HYSEP method (Sloto & Crouse 1996), and UKIH method (Piggott *et al.* 2005). The baseflow sequences obtained via these methods are usually not sufficiently smooth, which does not accurately reflect the actual situation. The second category involves the use

doi: 10.2166/ws.2019.074

of low-pass filters, corresponding to methods such as the Lyne–Hollick method (Lyne & Hollick 1979), Chapman–Maxwell method (Chapman 1999), and Eckhardt method (Eckhardt 2005, 2008), which are based on advances in signal processing. Such methods often require the determination of the recession constant and BFI_{max} (Eckhardt 2008). The low-pass filter methods have no obvious physical meaning corresponding to stream basins, and those methods cannot reasonably reflect actual hydrogeological conditions. In general, these methods need to be calibrated based on the mass balance method (Lott & Stewart 2016). The third category is composed of the mass balance methods, which use natural environmental tracers to separate the baseflow based on the mass balance equation (Cey *et al.* 1998; Cartwright *et al.* 2014). These methods usually require monitoring of the concentrations of tracers (ions, isotopes, conductivity, etc.) in surface runoff, stream water, and groundwater, and tracers in different basins can perfectly reflect the hydrogeological conditions. The separation results based on mass balance methods can reasonably accurately present the actual situation. However, a large amount of testing is required for the baseflow separation of large basins along with long-time-period records (Zhang *et al.* 2017).

In this context, Stewart *et al.* (2007) first showed that conductivity can be used as a tracer for baseflow separation via field tests. The authors then applied the conductivity mass balance (CMB) baseflow separation method to 10 basins in the United States. Lott & Stewart (2013), substituting the power function relationship between conductivity and streamflow into the CMB equation, derived the CMB power function (CMBPF) baseflow separation method. Lott & Stewart (2016) subsequently applied the CMB and CMBPF methods to 35 basins in the United States and corrected five conventional baseflow separation methods.

Conductivity, as a relatively easy-to-obtain tracer, has been favored by many hydrologists (Miller *et al.* 2014). However, many hydrological stations in the United States and other countries do not have historical records of conductivity, and thus, the application of the CMB and CMBPF methods has been limited. Thus, the search for a more common and low-cost tracer to substitute for conductivity has attracted considerable research interest.

Meanwhile, gage heights are recorded in almost all hydrological stations and can, therefore, be a more common tracer for baseflow separation. Against this backdrop, the main purpose of this study is to analyze the relationship between gage height and streamflow and to derive a mass balance method using gage height as a tracer (GHMB) and a power function method based on the gage height (GHPF).

In the study, the GHMB and GHPF methods were corrected by comparing the results of the CMB, CMBPF, GHMB, and GHPF methods in 20 basins in the United States. The corrected GHMB and GHPF methods were applied to seven other basins, and the effectiveness of the two methods was verified by comparison with conventional methods and the CMB method.

METHODS

CMB and CMBPF methods

CMB method

The CMB method has been derived from the two-component mass balance equation using conductivity as a tracer (Stewart *et al.* 2007):

$$Q_{BF} = \frac{Q(Q_C - RO_C)}{BF_C - RO_C} \tag{1}$$

where Q denotes the discharge (ft^3/s), Q_{BF} the baseflow (ft^3/s), Q_C the specific conductance, BF_C the baseflow conductivity, and RO_C the surface runoff conductivity.

CMBPF method

The CMBPF method is derived by substituting the power function equation $Q_C = a'Q^{b'}$ between discharge and conductivity into the CMB equation (Equation (1)) (Lott & Stewart 2013). Here, a' denotes the y-intercept of the best-fit straight line of the conductivity vs discharge plot in the double logarithmic coordinate system, and b' denotes the slope:

$$Q_{BF} = aQ^b + cQ \tag{2}$$

where a, b, and c are constants defined, respectively, as

$$a = \frac{a'}{BF_C - RO_C} \quad (3)$$

$$b = 1 + b' \quad (4)$$

$$c = -\frac{RO_C}{BF_C - RO_C} \quad (5)$$

Gage height as tracer

It is well known that there is a positive correlation between the gage height and discharge. As the discharge increases, the gage height also increases, and the synchronization between these two quantities is well studied (Appendix, Figure S1(a), available with the online version of this paper). The scatter points of the gage height vs discharge approximate a straight line in the double logarithmic coordinate system, which satisfies the power function of $H = aQ^b$ (also known as the rating curve). There is a positive correlation between gage height and discharge, and the slope of the gage height vs discharge curve is positive (Appendix, Figure S2(a), available online).

Simultaneously, conductivity is significantly reduced with increase in discharge, and the minimum conductivity values are very close for various flood peaks (Appendix, Figure S1(b)). In this regard, Lott & Stewart (2013) pointed out that the scatter points of conductivity vs discharge approximate a straight line in the double logarithmic coordinate system, which satisfies the power function of $Q_C = aQ^b$. Due to the negative correlation between conductivity and discharge, the slope of the line is negative (Appendix, Figure S2(b)).

The relationship between gage height and discharge is very similar to the relationship between conductivity and discharge. The measurement of gage height is easy to achieve, and many gages store the daily average data of gage height. Therefore, it is possible to utilize the gage height as a tracer for baseflow separation by appropriate conversion.

GHMB and GHPF methods

GHMB method

The gage height mass balance (GHMB) method has been derived using the gage height as a tracer via the two-component mass balance equation based on the assumption that the maximum gage height (H_{MAX}) can reflect the flooding feature and that the minimum gage height (H_{MIN}) can reflect the baseflow characteristics. The GHMB equation can be derived by replacing parameters RO_C, BF_C, and Q_C in Equation (1) with H_{MAX}, H_{MIN}, and H, respectively:

$$Q_{BF} = Q\frac{H_{MAX} - H}{H_{MAX} - H_{MIN}} \quad (6)$$

In order to facilitate the calibration of the gage height mass balance method, a correction factor k was added to Equation (6):

$$Q_{BF} = kQ\frac{H_{MAX} - H}{H_{MAX} - H_{MIN}} \quad (7)$$

where Q denotes the discharge (ft^3/s), Q_{BF} the baseflow (ft^3/s), H_{MAX} the maximum gage height (m), H_{MIN} the minimum gage height (m), H the gage height (m), and k the correction factor. Before calibration, k was set as 1. An accurate calibration factor was determined by the correlation between the results of CMB and GHMB.

GHPF method

The GHMB method requires continuous gage-height observations. In order to utilize limited gage height for long-period baseflow separation, the gage-height-based power function (GHPF) method has been derived by substituting the power function ($H = \alpha' Q^{\beta'}$) into the GHMB equation.

Upon rewriting Equation (6):

$$Q_{BF} = Q\frac{H_{MAX}}{H_{MAX} - H_{MIN}} - Q\frac{H}{H_{MAX} - H_{MIN}} \quad (8)$$

The gage height is related to discharge as

$$H = \alpha' Q^{\beta'} \quad (9)$$

where α' and β' denote the y-intercept and slope, respectively, of the best-fit straight line of the gage height vs discharge

scatter points in the log–log coordinate system. Substituting Equation (9) into Equation (8),

$$Q_{BF} = Q\frac{H_{MAX}}{H_{MAX} - H_{MIN}} - Q\frac{\alpha' Q^{\beta'}}{H_{MAX} - H_{MIN}} \quad (10)$$

Further,

$$Q_{BF} = -\frac{\alpha'}{H_{MAX} - H_{MIN}}Q^{\beta'+1} + \frac{H_{MAX}}{H_{MAX} - H_{MIN}}Q \quad (11)$$

Simplifying,

$$Q_{BF} = \alpha Q^{\beta} + \gamma Q \quad (12)$$

In order to facilitate the calibration of the gage-height-based power function method, a correction factor k was added to Equation (12). Before calibration, k was set as 1. Thus,

$$Q_{BF} = k(\alpha Q^{\beta} + \gamma Q) \quad (13)$$

where α, β, and γ are constants defined, respectively, as:

$$\alpha = -\frac{\alpha'}{H_{MAX} - H_{MIN}} \quad (14)$$

$$\beta = \beta' + 1 \quad (15)$$

$$\gamma = \frac{H_{MAX}}{H_{MAX} - H_{MIN}} \quad (16)$$

Data

This study uses data from 27 stream gages distributed across the USA. Basins that represent a large range of basin areas and physiographic and climatic regions were selected for the study. All the streams considered in this study are perennial streams, with basin areas ranging from 10 km^2 to 16,757 km^2. Each gage has at least 2 years of continuous discharge, specific conductance, and gage height over the same period. All discharge, gage height, and specific conductance data are daily average values retrieved from the United States Geological Survey's (USGS) National Water Information System (NWIS) website (http://waterdata.usgs.gov/nwis).

RESULTS AND DISCUSSION

Calibration of GHMB and GHPF methods

The average baseflow of the 20 basins separated by GHMB and GHPF methods is generally larger than that separated by the CMB and CMBPF methods. The average correlation coefficients of the four methods are greater than 0.75 (Appendix, Table S1, available with the online version of this paper). The correlation coefficients between daily baseflow for each gage as calculated by the GHMB and CMB methods range from 0.53 to 0.97 with an average of 0.78. The correlation coefficients between GHPF and CMBPF range from 0.34 to 1 with an average of 0.89. The correlation coefficients between GHPF and GHMB range from 0.73 to 0.99 with an average of 0.88. Further, the correlation coefficients between CMBPF and CMB are 0.37 to 0.99 with an average of 0.75. There are no obvious regularity changes between the correlation coefficients in different drainage areas. The high correlation and the closeness of the ratios indicate that it is reasonable to calibrate the GHMB and GHPF methods using a single constant k.

In the Cartesian coordinate system, the slope of the least-squares fit line for the average baseflow as calculated by GHPF and CMB is 0.55, with $R^2 = 0.85$ (Figure 1(a)). The slope of the least-squares fit line for the average baseflow as calculated by GHMB and CMB is 0.58, with $R^2 = 0.87$ (Figure 1(b)). Therefore, the values of the correction factor k for the GHPF and GHMB methods are 0.55 and 0.58, respectively.

The daily average baseflow values of the 20 basins were re-separated with the use of the calibrated GHMB and GHPF methods ($k = 0.58$ and 0.55). The average deviation of the baseflow from those of the calibrated GHMB and CMB methods was reduced to 17%. Further, the average deviation between the calibrated GHPF and CMB methods was reduced to 28%.

Application of corrected GHMB and GHPF methods to seven other basins

Comparison with conventional methods

The corrected GHMB, GHPF, CMB, and CMBPF methods were applied to seven other basins. The BFIs calculated in this study were compared with those calculated by Lott &

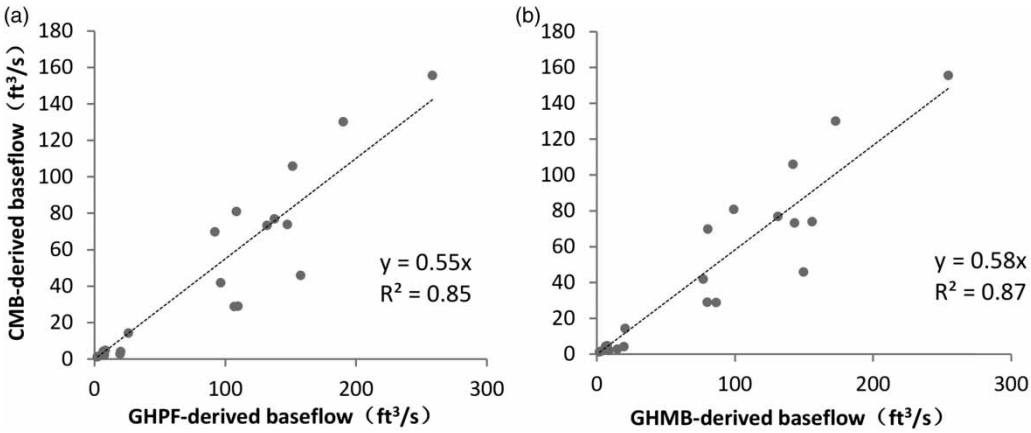

Figure 1 | Plots of (a) CMB-derived and GHPF-derived, (b) CMB-derived and GHMB-derived baseflows. The dotted line indicates the least-squares fit of the scatter point. Here, 1 $ft^3/s = 0.028\ m^3/s$.

Stewart (2016) with the use of different methods for the same basins (Table 1). The average BFI values calculated as per the corrected GHMB and GHPF methods were 0.33 and 0.37, respectively, and the average BFI obtained as per Lott & Stewart (2016) with the use of different methods ranged between 0.30 and 0.37. The GHMB and GHPF results exhibit good agreement with those of conventional methods.

Comparison with CMB method

Considering the CMB method as the standard, this study statistically analyzed the daily average baseflow calculated via the GHMB and GHMB methods after correction (Tables 2 and 3). The parameters of correlation coefficient (R), root-mean-square error (RMSE), scatter index (SI), BIAS, and Nash–Sutcliffe efficiency coefficient (NSE) were used (detailed definitions and formulae can be found in Lee *et al.* (2014), Najafzadeh & Zahiri (2015), Zahiri & Najafzadeh (2017), and Najafzadeh & Zeinolabedini (2018)).

The correlation coefficient (R) between the GHMB and CMB methods ranges between 0.51 and 0.86, while the NSE ranges between 0.11 and 0.73 (Table 2). The R value between the GHPF and CMB methods lies between 0.62 and 0.84, and the NSE is between −1.61 and 0.63 (Table 3). The daily average baseflow as calculated by the GHMB and GHPF methods can be suitably fitted with the CMB method, but the GHMB method is closer to the CMB method than the GHPF method.

Figure 2 shows the cumulative baseflow obtained from the GHMB, GHPF, CMB, and CMBPF methods. The

Table 1 | BFI for seven other basins in the United States as calculated from corrected GHMB and GHPF methods and CMB, CMBPF, HYSEP (sliding), WHAT, and BFI2 methods; 1 $mi^2 = 2.59\ km^2$

				BFI as per this study				BFI of Lott & Stewart (2016)			
State	Gage number	Period of record	Area (mi^2)	GHMB	GHPF	CMB	CMBPF	CMB	HYSEP (sliding)	WHAT	BFI2
FL	2300500	1973/11–1977/9	149	0.20	0.23	0.14	0.13	0.15	0.18	0.15	0.21
FL	2297100	2001/12–2010/4	132	0.27	0.31	0.24	0.25	0.21	0.51	0.22	0.23
GA	2336300	2010/11–2014/9	86.8	0.36	0.42	0.37	0.36	0.37	0.39	0.38	0.33
SC	2160105	2010/11–2014/9	759	0.38	0.42	0.33	0.33	0.35	0.38	0.35	0.51
SC	2160700	2010/11–2014/9	444	0.38	0.40	0.28	0.28	0.29	0.38	0.30	0.34
MO	6894000	2010/11–2014/9	184	0.26	0.27	0.21	0.22	0.14	0.14	0.14	0.15
KS	7144780	2015/12–2017/11	713	0.47	0.51	0.55	0.54	0.62	0.60	0.61	0.62
Mean				0.33	0.37	0.30	0.30	0.30	0.37	0.31	0.34
Standard error of the mean				0.01	0.01	0.02	0.02	0.03	0.03	0.03	0.03

Table 2 | Statistical analysis of daily baseflow obtained from GHMB and CMB methods

Gage number	*R*	RMSE	SI	BIAS	NSE
2300500	0.51	5.50	0.73	−0.31	0.30
2297100	0.86	16.32	0.64	−1.27	0.62
2336300	0.68	18.04	0.94	−1.57	0.43
2160105	0.78	69.41	0.41	−24.17	0.11
2160700	0.78	46.01	0.38	−13.58	0.17
6894000	0.86	19.13	0.79	0.43	0.73
7144780	0.79	29.47	0.51	−0.05	0.63

Table 3 | Statistical analysis of daily baseflow obtained from GHPF and CMB methods

USGS gages	*R*	RMSE	SI	BIAS	NSE
2300500	0.62	5.49	0.73	−0.18	0.30
2297100	0.84	16.17	0.64	−1.33	0.63
2336300	0.79	18.73	0.98	0.06	0.39
2160105	0.82	103.08	0.60	−13.28	−0.87
2160700	0.81	81.42	0.67	−0.23	−1.61
6894000	0.79	30.33	1.26	1.97	0.31
7144780	0.77	32.19	0.55	−10.38	0.56

cumulative errors of the separation results of the four methods in different basins are small. The same trend and smaller deviation indicate the effectiveness of gage height as a tracer.

Separation results of single flood events

When the flood peak is smaller, the baseflow fluctuates positively with the streamflow, and the baseflows calculated as per the GHMB, GHPF, and CMB methods exhibit the same fluctuation trend. In the early stage of recession, the baseflow as calculated by the GHMB and GHPF methods is slightly larger than that calculated by the CMB method (Figure 3(a)).

When the flood peak is larger, the baseflow as calculated by the GHMB and CMB methods is obviously suppressed and that of the GHMB method is more obvious, while the GHMB method affords no obvious suppression (Figure 3(b)). When the flood peak is larger, the gage height of the river is higher than the groundwater level, the river water leaks into the groundwater aquifer, and thus, the baseflow is suppressed (Lott & Stewart 2013).

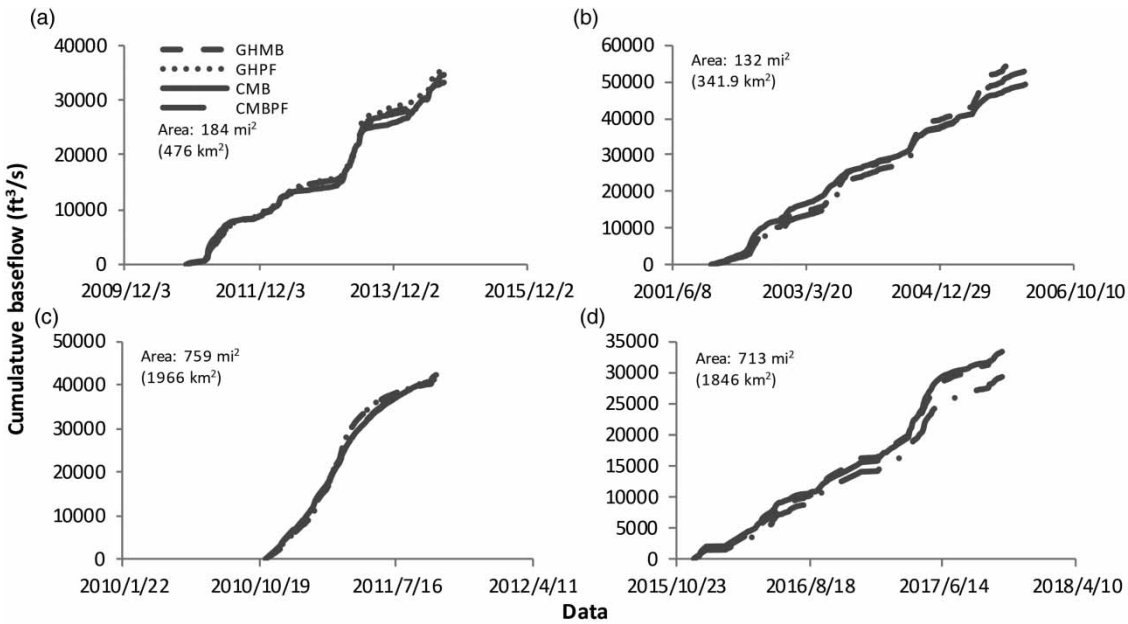

Figure 2 | Cumulative plots of CMB-derived, CMBPF-derived, GHMB-derived, and GHPF-derived baseflows after calibration: (a) USGS gage number 06894000, (b) USGS gage number 02297100, (c) USGS gage number 02160105, (d) USGS gage number 07144780; data are daily averages; 1 $ft^3/s = 0.028\ m^3/s$ and 1 $mi^2 = 2.59\ km^2$.

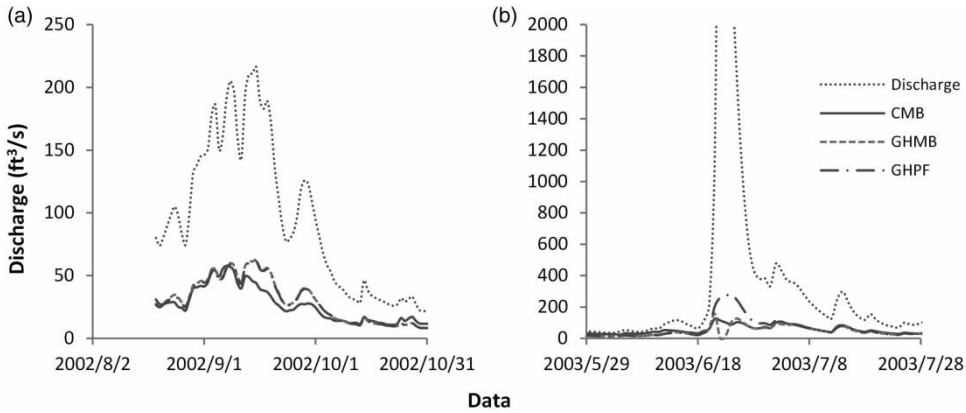

Figure 3 | Baseflows of single flood events in basin with USGS site number 02297100: (a) smaller peak and (b) larger peak; 1 $ft^3/s = 0.028\ m^3/s$.

The separation results of the GHMB, GHPG, and CMB methods are highly consistent in the low-flow stage, and therefore, the deviation of baseflow between the gage height and conductivity as tracers mainly occurs in flood events, particularly when the flood peak is large.

CONCLUSIONS

Upon using the gage height as tracer, this study derived the GHMB (Equation (7)) and GHPF (Equation (13)) methods by means of the two-component mass balance equation. The GHMB and GHPF methods were corrected by comparing the results of the CMB, CMPF, GHMB, and GHPF methods for 20 basins in the United States. The application of the corrected GHMB and GHPF methods to seven other basins enabled the following conclusions to be drawn:

(1) The BFI values calculated as per the GHMB and GHPF methods ranged as 0.20–0.47 and 0.23–0.51, respectively, which were in good agreement with the corresponding ranges of the conventional methods.
(2) The statistical analysis results showed that the GHMB and GHPF methods can be well fitted with the CMB method (the mean R values were 0.75 and 0.78, and the NSE means were 0.43 and −0.04, for GHMB and GHPF, respectively).
(3) The results of baseflow separation during flood events indicate that the baseflow is significantly suppressed when the flood peak is larger, and the deviation between the GHMB, GHPF, and CMB methods mainly occurs in the case of flood events with a large flood peak.

In this study, the GHMB and GHPF methods were corrected using a single constant k, which may not be applicable for individual basins. For example, for basins with USGS gage numbers 2160105 and 2160700, the NSE values were relatively small (the GHMB method afforded values of 0.11 and 0.17, while the GHPF method afforded values of −0.87 and −1.61, respectively).

Future studies will need to focus on correcting the GHMB and GHPF methods with the use of varying coefficients, and special attention needs to be paid to the correction of deviations in flood events. In conclusion, the findings of this study can suitably contribute to developments in hydrology.

ACKNOWLEDGEMENTS

This work was supported by the National Natural Science Foundation of China (41572216); the Provincial School Co-construction Project Special – Leading Technology Guide (SXGJQY2017-6); and the Jilin Province Key Geological Foundation Project (2014–13). We would like to thank all anonymous reviewers whose suggestions greatly improved this manuscript.

DECLARATIONS OF INTEREST

None.

REFERENCES

Bahrami, E., Mohammadrezapour, O., Salarijazi, M. & Jou, P. H. 2019 Effect of base flow and rainfall excess separation on runoff hydrograph estimation using gamma model (case study: Jong catchment). *KSCE Journal of Civil Engineering* **23** (3), 1420–1426.

Bastola, S., Seong, Y., Lee, D., Youn, I., Oh, S., Jung, Y., Choi, G. & Jang, D. 2018 Contribution of baseflow to river streamflow: study on Nepal's Bagmati and Koshi basins. *KSCE Journal of Civil Engineering* **22** (11), 4710–4718.

Cartwright, I., Gilfedder, B. & Hofmann, H. 2014 Contrasts between estimates of baseflow help discern multiple sources of water contributing to rivers. *Hydrology and Earth System Sciences* **18** (1), 15–30.

Cey, E. E., Rudolph, D. L., Parkin, G. W. & Aravena, R. 1998 Quantifying groundwater discharge to a small perennial stream in Southern Ontario, Canada. *Journal of Hydrology* **210** (1–4), 21–37.

Chapman, T. 1999 A comparison of algorithms for stream flow recession and baseflow separation. *Hydrological Processes* **13** (5), 701–714.

Eckhardt, K. 2005 How to construct recursive digital filters for baseflow separation. *Hydrological Processes* **19** (2), 507–515.

Eckhardt, K. 2008 A comparison of baseflow indices, which were calculated with seven different baseflow separation methods. *Journal of Hydrology* **352** (1–2), 168–173.

Lee, G., Shin, Y. & Jung, Y. 2014 Development of web-based RECESS model for estimating baseflow using SWAT. *Sustainability* **6** (4), 2357–2378.

Lott, D. A. & Stewart, M. T. 2013 A power function method for estimating base flow. *Ground Water* **51** (3), 442–451.

Lott, D. A. & Stewart, M. T. 2016 Base flow separation: a comparison of analytical and mass balance methods. *Journal of Hydrology* **535**, 525–533.

Lyne, V. & Hollick, M. 1979 Stochastic time-variable rainfall-runoff modeling. In: *Institute of Engineers Australia National Conference*, pp. 89–93.

Miller, M. P., Susong, D. D., Shope, C. L., Heilweil, V. M. & Stolp, B. J. 2014 Continuous estimation of baseflow in snowmelt-dominated streams and rivers in the Upper Colorado River Basin: a chemical hydrograph separation approach. *Water Resources Research* **50** (8), 6986–6999.

Najafzadeh, M. & Zahiri, A. 2015 Neuro-fuzzy GMDH-based evolutionary algorithms to predict flow discharge in straight compound channels. *Journal of Hydrologic Engineering* **20** (12), 04015035.

Najafzadeh, M. & Zeinolabedini, M. 2018 Derivation of optimal equations for prediction of sewage sludge quantity using wavelet conjunction models: an environmental assessment. *Environmental Science & Pollution Research* **25** (23), 22931–22943.

Piggott, A. R., Moin, S. & Southam, C. 2005 A revised approach to the UKIH method for the calculation of baseflow. *Hydrological Sciences Journal* **50** (5), 911–920.

Saraiva Okello, A. M. L., Uhlenbrook, S., Jewitt, G. P. W., Masih, I., Riddell, E. S. & Van der Zaag, P. 2018 Hydrograph separation using tracers and digital filters to quantify runoff components in a semi-arid meso-scale catchment. *Hydrological Processes* **32**, 1334–1350.

Sloto, R. A. & Crouse, M. Y. 1996 *HYSEP: A Computer Program for Streamflow Hydrograph Separation and Analysis*. US Geological Survey Water-Resources Investigations Report 96-4040, Lemoyne, PA, USA.

Stewart, M., Cimino, J. & Ross, M. 2007 Calibration of base flow separation methods with streamflow conductivity. *Ground Water* **45** (1), 17–27.

Wahl, K. L. & Wahl, T. L. 1988 Effects of regional groundwater level declines on streamflow in the Oklahoma Panhandle. In: *Proceedings of the Symposium on Water-Use Data for Water Resources Management*, American Water Resources Association, Middleburg, VA, USA, pp. 239–249.

Zahiri, A. & Najafzadeh, M. 2017 Optimized expressions to evaluate the flow discharge in main channels and floodplains using evolutionary computing and model classification. *International Journal of River Basin Management* **16** (1), 123–132.

Zhang, L., Brutsaert, W., Crosbie, R. & Potter, N. 2014 Long-term annual groundwater storage trends in Australian catchments. *Advances in Water Resources* **74**, 156–165.

Zhang, J., Zhang, Y., Song, J. & Cheng, L. 2017 Evaluating relative merits of four baseflow separation methods in Eastern Australia. *Journal of Hydrology* **549**, 252–263.

First received 9 September 2018; accepted in revised form 7 May 2019. Available online 20 May 2019